UNITECH SELECTED PAPERS

International Scientific Conference
UNITECH`2024

INVESTIGATION OF THE EFFECT OF COOLING RATE ON THE MICROSTRUCTURE EVOLUTION OF STRONTIUM: A MOLECULAR DYNAMICS SIMULATION STUDY

Murat Celtek[1*], Unal Domekeli[2]

[1]*Faculty of Education, Trakya University, 22030, Edirne – TÜRKİYE*
[2]*Dept. of Physics, Trakya University, 22030, Edirne – TÜRKİYE*

** Corresponding author: mceltek@trakya.edu.tr*

Abstract

In the present study, the microstructure evolution of melt strontium (Sr) element cooled with different cooling rates has been investigated by molecular dynamics (MD) simulations. In order to describe the interactions between atoms in the system, the embedded atom method (EAM) potential, which is widely used in metallic systems in the literature, is preferred. All MD simulations have been performed with the DLPOLY 2.0 open source package. The pair distribution function (PDF) and structure factor (SF) obtained from EAM-MD simulations for liquid Sr during the cooling process are in good agreement with experimental results in the literature. It has been observed that the cooling rate had significant effects on the structural change of Sr. When the system has been cooled more slowly, liquid-crystalline phase transitions have been observed at different temperature points, while when cooled more rapidly, disorder prevailed in the system and ultimately amorphous structures have been formed. It is believed that the present findings will contribute to the literature in understanding what kind of changes occur in the microstructure of Sr element solidified with different cooling rates.

Keywords: strontium, embedded atom potential, cooling rates, microstructure, molecular dynamics simulations.

INTRODUCTION

As is known, Calcium is one of the most abundant substances in the earth's crust. That is why it has always managed to attract the attention of scientists, and has been studied extensively compared to other alkaline earth metals [1]. On the other hand, Strontium (Sr) deserves attention because it is a semimetal, located between its two vertical neighbors, Calcium and Barium, and has the physical and chemical properties of them. Sr has a very wide range of uses, some of which are; high voltage television tubes, automotive industry, iron ore separators, photocopy machines, special alloys and many more. Its compounds, strontium sulfide, are used in fireworks and paints. Strontium nitrate is used in the pharmaceutical industry and in fireworks to give the flame a dark color [4]. Understanding how elements behave under different conditions plays a leading role in the discovery of new alloys and materials formed by combining many elements. In the present study, we investigated the effects of cooling rate on the microstructure of molten Sr using classical MD simulations performed with the DL_POLY 2.0 open source software package [2]. The interactions between Sr atoms were modeled using the EAM potential generated by H.W. Sheng [3]. Results regarding this potential have been reported in previous studies, please see Ref [4] for more detailed information. Volume-temperature (V-T) curves were used to examine behaviors such as liquid-amorphous or liquid-crystal transitions of the rapidly solidified system. Moreover, in order to see and discuss the changes occurring in the microstructure of the system in more detail during this process, PDF and the Honeycutt-Andersen (HA) method [5] have been adopted. Brief information about these methods will be given in the following sections.

EXPOSITION

The preferred EAM potential considers the embedding in the local electron density of neighboring atoms in the Sr metal and finally

doi: www.doi.org/10.70456/.....

calculates the energy of each atom in the system. The total energy is calculated using the equation given below [6,7]:

$$\mathbf{E_{tot}} = \sum_i \mathbf{F_i}(\rho_i) + \frac{1}{2}\sum_{i\neq j} \Phi_{ij}(\mathbf{r_{ij}}) \qquad (1)$$

In this relation, Φ_{ij} represents the pair interaction energy between atoms i and j at a distance r_{ij} . F_i is the embedding energy of an atom i in a local site characterized by an electron density ρ_i and the electron density can be determined as follows.

$$\rho_i = \sum_{j,\ j\neq i} \mathbf{f_j}(\mathbf{r_{ij}}) \qquad (2)$$

where $f_j(r_{ij})$ corresponds to the electron density at position i atom originating from an atom j located at distance r_{ij}. The time step was chosen as t=0.001 ps and the periodic boundary conditions were applied to all three directions of the simulation box. There are a total of 6912 Sr atoms in the cubic cell. Berendsen thermostat and barostat were used to control the temperature and pressure, respectively, throughout the simulations. The equations of motion were solved using the Leap-Frog algorithm. OVITO program [8] has been used for visualization and HA analyses. First, the system was obtained as a liquid at 2000 K, which is sufficiently higher than the experimental melting point of Sr (T_m^{exp} = 1042 K) [9]. Then, simulations were carried out under the isobaric isothermal ensemble (NPT) with different cooling rates (γ_1=20 Kps^{-1}, γ_2=5 Kps^{-1}, γ_3=1 Kps^{-1} and γ_4=0.1 Kps^{-1}) by cooling 50 K temperature steps from 2000 K to 100 K. In order to see the effect of the cooling rate on the transition process, the volume per atom curves as a function of temperature (V-T) are shown in Fig.1. In general, the first thing that is noticeable is that the volume of the system decreases with decreasing temperature for all cooling rates, as expected. At high temperatures (700 K and above), the V-T curves obtained from four cooling rates almost overlap each other. This is an indication that the system is stable in liquid form in this temperature range. As can be seen from the figure, we observe two different situations for cooling rates of γ_1=20 Kps^{-1}-γ_2=5 Kps^{-1} and γ_3=1 Kps^{-1}-γ_4=0.1 Kps^{-1}. First, for relatively high cooling rates (γ_1=20 Kps^{-1} and γ_2=5 Kps^{-1}), the volume continues to decrease continuously towards lower temperatures, while only a slight change in the slope of the V-T curve is observed. This shows us that at the relevant cooling rates, liquid-glass transition occurs in the system, or in other words, crystallization does not occur. Secondly, we observe that for lower cooling rates (γ_3=1 Kps^{-1} and γ_4=0.1 Kps^{-1}) a sudden jump in the volume of the system occurs at low temperatures. Moreover, when the time allowed for the system to cool was increased, we observed that the liquid-crystal transition occurred at higher temperatures. This shows us that the atoms have locally returned to their crystalline order, which we confirmed with atomic visualizations obtained at 300 K for all cooling rates shown in Fig.2. From the figure, we see that for γ_1=20 Kps^{-1} and γ_2=5 Kps^{-1} the atoms are randomly distributed similar to liquid structures, while for γ_3=1 Kps^{-1} and γ_4=0.1 Kps^{-1} cooling rates the atoms are arranged in a certain order.

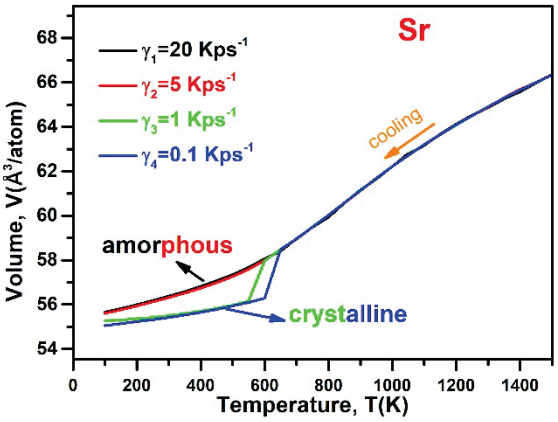

Fig.1. *Change of volume with decreasing temperature during the cooling process for four different cooling rates.*

We adopted the pair distribution function (PDF or g(r)) to study the structural characterization of the system during the cooling process. PDF analysis is one of the most preferred methods in the process of characterizing the local structure of the system in MD simulation studies. For more detailed information about this method, please see Ref [10–12].

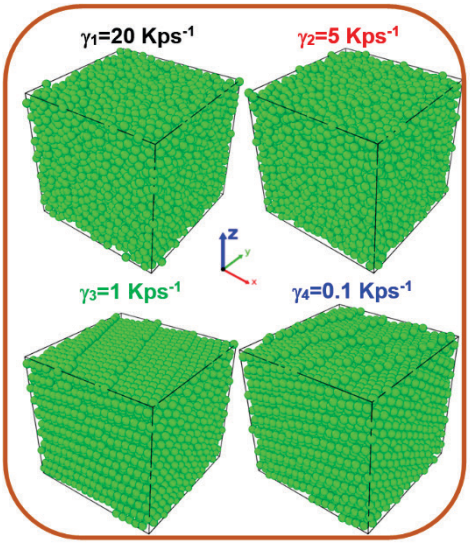

Fig. 2. *Snapshots of simulation boxes at 300 K for different cooling rates.*

To avoid repetition, the g(r) curves obtained at different temperatures with only γ_1=20 Kps^{-1} and γ_4=0.1 Kps^{-1} cooling rates where the crystal and amorphous structure have been obtained are shown in Figs. 3(a-b). The g(r) curves obtained at temperatures of 700 K and above for both cooling rates exhibit the typical properties of liquid structures. Moreover, with decreasing temperature, the height of the first peaks of g(r) increases and their width decreases. This is an indication that the atomic order in the first coordination shell increases with decreasing temperature and short-range order (SRO) develops. As the temperature decreases further, a clear difference is observed in the peaks of the g(r) curves obtained from both cooling rates. As can be seen from Fig.3(a), there is a splitting in the second peak of the g(r) curves obtained for the faster cooled system, which becomes more pronounced with decreasing temperature. This behavior is characteristic for amorphous materials and is an indication of the development of SRO and medium-range order (MRO) in the system. The results in Figure 3(b) show that the g(r) curves obtained at temperatures below 500K for the slower cooled system produce sharp peaks typical of crystal structures. This shows that there is enough time for crystal nuclei to form and develop in the slower cooled systems.

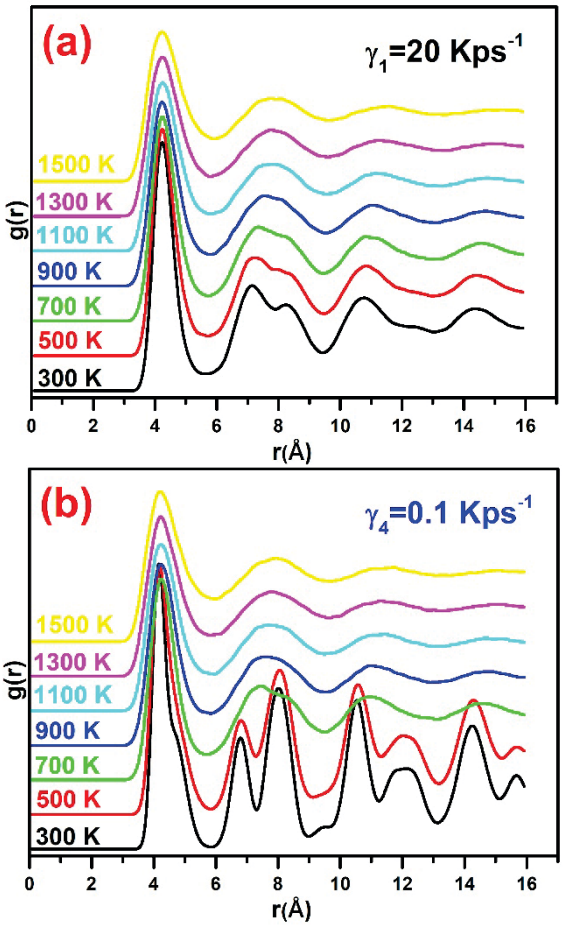

Fig. 3. *PDF curves obtained at different temperatures for the system cooled with (a) γ_1=20 Kps^{-1} and (b) γ_4=0.1 Kps^{-1} cooling rates.*

To check the reliability of the selected EAM potential, we compared the g(r) and structure factors (SF or S(q)) calculated from EAM-MD simulations at 1050 K with the experimental data at 1043 K [13]. The results in Fig. 4 depict that there is excellent agreement between the simulation and experimental results. Even for the second and third peaks, the calculated g(r)'s can perfectly reproduce the experimental data. This good agreement reveals that the microscopic model we adopted is successful in describing the interatomic interactions in the pure Sr system and produces reliable results.

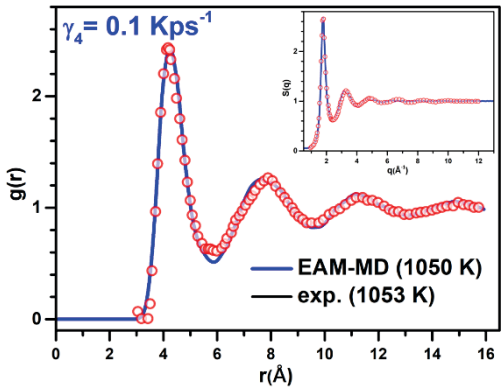

Fig. 4. *Comparison of EAM-MD simulation results and experimental data for liquid Sr.*

We used HA bond-type index [5] to more accurately follow the changes in the microstructure of the system under different cooling rates. HA bond-type index is a useful analysis method that can classify the states of neighboring atoms surrounding the considered atom pair and their bonds with each other. According to this classification, the index of 1551 represents the ideal icosahedral structure, while the indexes of 1431 and 1541 represent the defect icosahedral structure. While the 1421 index is characteristic of fcc crystal structures, the 1421+1422 indexes are characteristic of hcp structures. The 1661 and 1441 indexes are associated with bcc crystal structures. For more information on the HA analysis method, please see Ref [14–16]. Figs. 5(a-g) depict the changes in the relative fractions of the main bonded pairs prevalent in amorphous and crystalline structures obtained under different cooling rates as a function of temperature. HA analysis results show that the most dominant pairs in liquid Sr for all cooling rates are 1431, 1541 and 1551 bonded pairs. HA analysis results obtained from γ_1=20 Kps^{-1} and γ_2=5 Kps^{-1} cooling rates show that the 1551 bonded pairs increase significantly with decreasing temperature. Another indicator of the development of icosahedral order, the 1431 and 1541 bonded pairs, change slightly at high temperatures and start to decrease around 700 K, which corresponds to the region where the distribution of 1551 bonded pairs increases the most. While the distribution of 1421, 1422, 1441 and 1661 bonded pairs, which are indicative of other crystal structures, is very little visible for these cooling rates, a slight change is again observed around 700 K. All the findings show us that the degree of icosahedral arrangement in the system shows a remarkable increase and its structure remains stable in the amorphous state. While the HA analysis results obtained from γ_3=1 $Kps^{-1}$and γ_4=0.1 Kps^{-1} cooling rates exhibited similar behavior to the results obtained from other cooling rates for high temperatures, much more pronounced and different changes have been observed compared to the amorphous structure at lower temperatures. What is most noticeable here is the sudden increase in the fraction of 1441 and 1661 bond pairs representing the bcc crystal structure at 550 K and 600 K for the cooling rates of γ_3=1 $Kps^{-1}$and γ_4=0.1 Kps^{-1}, respectively. As a result, the fraction of all other bonded pairs decreases abruptly in the same temperature ranges. This liquid-bcc crystal phase transition is also confirmed by the behavior of V-T and g(r) curves discussed in Fig. 1 and Fig. 3(b) respectively. Another important point is that the more time is given to the system to reach equilibrium, the higher the temperatures at which crystallization occurs. To make this process more concrete, the distributions and snapshots of the HA analysis results at 300 K temperature for each cooling rate are shown in Fig.6. As can be seen from the figure, in systems that are cooled more rapidly, the atoms are seen to adopt a random arrangement, while when the system is given more time to come to equilibrium, a very large proportion of the atoms now adopt the bcc crystal structure arrangement. The interesting thing here is that while the Sr element normally has an fcc crystal structure at room temperature, it undergoes a liquid-bcc phase transition during the rapid solidification process. This situation can be explained by the "step rule" proposed by Ostwald, which suggests that the first phase formed is not the one that is thermodynamically stable, but the one with the free energy closest to the liquid phase [17]. In addition, Pan et al. [18] observed that the bcc crystal structure is more liquid-like than other crystals from the perspective of atomic motion.

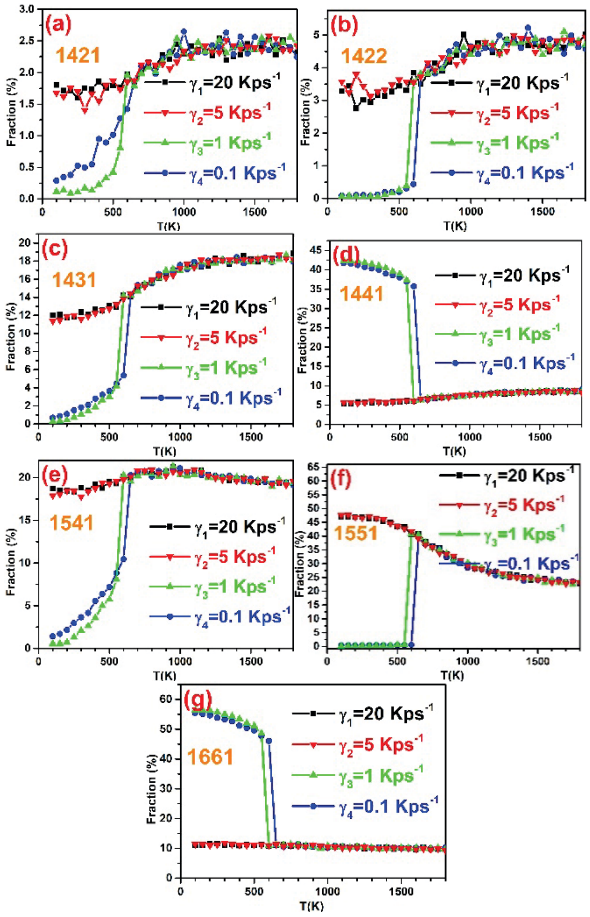

Fig.5. *Temperature dependent fraction of (a)1421, (b)1422, (c)1431, (d)1441, (e)1541, (f)1551 and (g)1661 bonded pairs calculated for different cooling rates.*

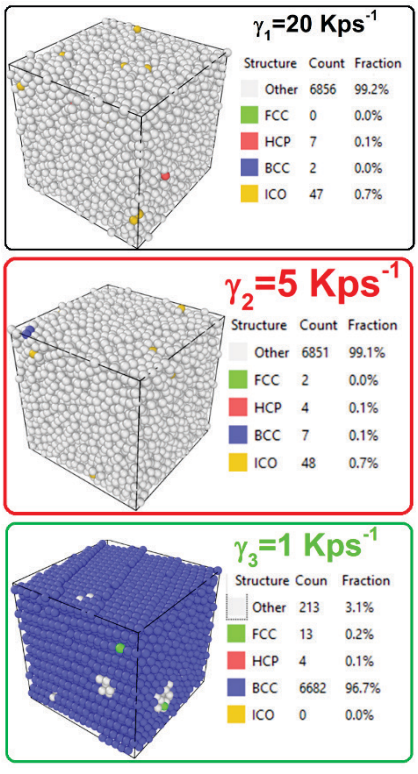

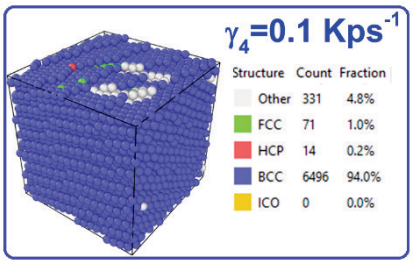

Fig. 6. *HA analysis results at 300K for different cooling rates.*

CONCLUSION

In summary, the amorphous formation, crystallization process and microstructure evolution of Sr cooled with different cooling rates have been investigated by EAM-MD simulations. It has been observed that the g(r) and S(q) curves calculated from EAM-MD simulations for liquid Sr have been in excellent agreement with the experimental data. Extensive statistical analysis has shown that when molten Sr is cooled faster (γ_1=20 Kps^{-1} and γ_2=5 Kps^{-1}), the system prefers disorder and eventually remains stable in an amorphous structure. In molten Sr, which is cooled more slowly (γ_3=1 Kps^{-1}and γ_4=0.1 Kps^{-1}), a liquid-bcc crystal phase transition is observed. It is believed that the present findings will shed light on the literature in understanding how Sr behaves under different conditions.

Funding: No funding support has been received from any institution or person.

Acknowledgments: We would like to thank Trakya University Rectorate for giving permission and contributing to present this study as a paper.

REFERENCE

[1] Chellathurai M, Gogovi GK, Papaconstantopoulos DA. Electronic structure and tight-binding molecular dynamics simulations for calcium and strontium. Materialia. 2020;14:100915.

[2] Smith W, Forester TR. DL_POLY_2.0: A general-purpose parallel molecular dynamics simulation package. Journal of Molecular Graphics. 1996;14(3):136–41.

[3] Sheng HW. Sr.lammps.eam. https://sites.google.com/site/eampotentials/sr

. 2024.
[4] Celtek M, Domekeli U, Sengul S. Strontıum Under High Pressure and Different Temperature Conditions: A Molecular Dynamics Simulation Study. In: International Scientific Conference. Gabrovo-Bulgaria; 2022. p. 328–32.
[5] Honeycutt JD, Andersen HC. Molecular Dynamics Study of Melting and Freezing of Small Lennard- Jones Clusters. Journal of Physical Chemistry. 1987;91(24):4950–63.
[6] Daw MS, Baskes MI. Embedded atom method: derivation and application to impurities,surfaces and other defects in metal. Phsical Review B. 1984;29(12):6443–53.
[7] Celtek M, Sengul S, Domekeli U, Guder V. Dynamical and structural properties of metallic liquid and glass Zr48Cu36Ag8Al8 alloy studied by molecular dynamics simulation. Journal of Non-Crystalline Solids. 2021;566:120890.
[8] Stukowski A. Visualization and analysis of atomistic simulation data with OVITO-the Open Visualization Tool. Modelling and Simulation in Materials Science and Engineering. 2010;18(1):015012.
[9] Kittel C. Introduction to Solid State Physics. New York: John Wiley & Sons Inc.; 1986.
[10] Celtek M. An in-depth investigation of the microstructural evolution and dynamic properties of Zr77Rh23 metallic liquids and glasses: a molecular dynamics simulation study. Journal of Applied Physics. 2022;132(3).
[11] Guder V, Celtek M, Celik FA, Sengul S. Crystallization analysis and determination of Avrami exponents during isothermal annealing and the effect of cooling rate on the evolution of the atomic structure of Pd78Si16Cu6 alloy: A molecular dynamics simulation study. Journal of Non-Crystalline Solids. 2023;602:122067.
[12] Celtek M. The effect of atomic concentration on the structural evolution of Zr100-xCox alloys during rapid solidification process. Journal of Non-Crystalline Solids. 2019;513:84–96.
[13] Waseda Y. The Structure of Non-Crystalline Materials-Liquids and Amorphous Solids. New York: London: McGraw-Hill; 1981.
[14] Guder V, Sengul S, Celtek M, Domekeli U. Pressure dependent evolution of microstructures in Pd80Si20 bulk metallic glass. Journal of Non-Crystalline Solids. 2022;576:121290.
[15] Celtek M, Sengul S, Domekeli U, Guder V. Molecular dynamics simulations of glass formation, structural evolution and diffusivity of the Pd-Si alloys during the rapid solidification process. Journal of Molecular Liquids. 2023;372:121163.
[16] Celtek M. Atomic structure of Cu60Ti20Zr20 metallic glass under high pressures. Intermetallics. 2022;143:107493.
[17] Ostwald W. Studien über die Bildung und Umwandlung fester Körper. Zeitschrift für Physikalische Chemie. 1897;22U(1):289–330.
[18] Pan SP, Feng SD, Qiao JW, Wang WM, Qin JY. Crystallization pathways of liquid-bcc transition for a model iron by fast quenching. Scientific Reports. 2015;5(1):16956.